AMERICAN SOCIETY of
GENE & CELL
THERAPY

AAV5-miHTT Gene Therapy Demonstrates Sustained Huntingtin Lowering and Functional Improvement in Huntington Disease Mouse Models

Elisabeth A. Spronck,[1] Cynthia C. Brouwers,[1] Astrid Vallès,[1] Martin de Haan,[1] Harald Petry,[1] Sander J. van Deventer,[1,2] Pavlina Konstantinova,[1] and Melvin M. Evers[1]

[1]Department of Research and Development, uniQure biopharma B.V., Amsterdam, the Netherlands; [2]Department of Gastroenterology and Hepatology, Leiden University Medical Center, Leiden, the Netherlands

Huntington disease (HD) is a fatal neurodegenerative disorder caused by an autosomal dominant CAG repeat expansion in the *huntingtin* (*HTT*) gene. The translated expanded polyglutamine repeat in the HTT protein is known to cause toxic gain of function. We showed previously that strong HTT lowering prevented neuronal dysfunction in HD rodents and minipigs after single intracranial injection of adeno-associated viral vector serotype 5 expressing a microRNA targeting human *HTT* (AAV5-miHTT). To evaluate long-term efficacy, AAV5-miHTT was injected into the striatum of knockin Q175 HD mice, and the mice were sacrificed 12 months post-injection. AAV5-miHTT caused a dose-dependent and sustained HTT protein reduction with subsequent suppression of mutant HTT aggregate formation in the striatum and cortex. Functional proof of concept was shown in transgenic R6/2 HD mice. Eight weeks after AAV5-miHTT treatment, a significant improvement in motor coordination on the rotarod was observed. Survival analysis showed that a single AAV5-miHTT treatment resulted in a significant 4-week increase in median survival compared with vehicle-treated R6/2 HD mice. The combination of long-term HTT lowering, reduction in aggregation, prevention of neuronal dysfunction, alleviation of HD-like symptoms, and beneficial survival observed in HD rodents treated with AAV5-miHTT supports the continued development of HTT-lowering gene therapies for HD.

INTRODUCTION

Huntington disease (HD) is a neurodegenerative disorder caused by a CAG trinucleotide repeat expansion in the first exon of the *huntingtin* (*HTT*) gene. This results in an expanded polyglutamine repeat in the HTT protein, causing toxic gain of function, affecting numerous cellular processes, and, ultimately, leading to neuronal death.[1] Disease onset usually occurs around 35–45 years of age, and symptoms are choreiform movement, impaired coordination, and psychiatric disturbances.[2] HD is a fatal disease, usually within 15 years after disease onset.[3] Brain areas that are affected most by the disease are the striatum and the motor cortex.[4] Clearance of the mutant HTT is currently accepted as being key for HD treatment and is the target of several different potential disease-modifying therapies.[5]

Since the discovery of the *HTT* gene, several groups have investigated HTT-lowering strategies such as antisense oligonucleotides (ASOs), RNAi, ribozymes, DNA enzymes, and genome-editing approaches.[6,7] One of the therapeutic approaches for HTT lowering acts through binding of molecules to *HTT* mRNA to block translation into the toxic HTT protein. ASOs have been shown to lower the amount of HTT protein in mouse models of HD, which leads to delayed disease progression and even reversal of the disease phenotype.[4,8,9] Currently, a phase I trial using repetitive intrathecal administration of ASOs in HD patients is ongoing.[10] Artificial small interfering RNAs (siRNAs), short hairpin RNAs (shRNAs), or microRNAs (miRNAs) bind to *HTT* mRNA and reduce its translation by the endogenous RNAi machinery.[11] Adeno-associated viral (AAV) vectors are the most common vehicles of choice to deliver the gene cassette containing RNAi, and a large number of AAV capsid serotypes provide cell- and tissue-specific tropism.[12] For the CNS, studies in rodents and non-human primates have shown AAV serotype 5 (AAV5) to effectively transduce the brain, making it an attractive candidate for RNAi-based gene transfer.[13–16] Our approach involves expression of a gene cassette encoding an engineered miRNA targeting human HTT, delivered via AAV5 (AAV5-miHTT) directly into the brain area affected most in HD, the striatum. This would allow continuous expression of therapeutic miRNAs after a single administration of the AAV vector, potentially resulting in long-term HTT lowering.

We previously showed a strong reduction of HTT in the brain of humanized HD mice,[17] prevention of neuronal dysfunction in lentiviral HD rats after a single intracranial injection of AAV5-miHTT,[18] and successful translation to the large HD minipig brain.[19] Here we investigated long-term HTT protein lowering, tolerability of AAV5-miHTT treatment, and functional improvement in Q175 knockin (KI) (heterozygous) HD mice[20] and R6/2 HD mice.[21] The models were chosen to investigate both the slow disease progression in
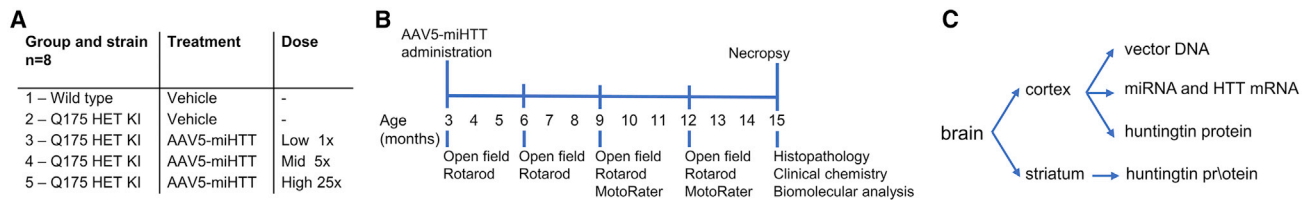
Figure 1. AAV5-miHTT Administration in the Mouse Brain Using a Single Bilateral Intrastriatal Stereotactic Injection

(A) Experimental setup (n = 8 per group) showing wild-type and Q175 KI mice used in the study with the different dose groups. (B) Experimental setup. Behavioral tests were performed to assess motor skills at several time points as indicated. Day of dosing (at 3 months of age) and necropsy (at 15 months of age) are also indicated. (C) Brain sampling overview. The striatum and cortex were dissected from the rest of the brain. The cortex was cryo-pulverized, and the powdered tissue was divided into three parts: one for vector DNA analysis, one for RNA analysis, and one for huntingtin protein analysis. The striatum was only used for huntingtin protein analysis.

Q175 mice as well as the rapidly developing phenotype seen in the R6/2 model. Both models were treated once with AAV-miHTT directly in the striatum. Dose-dependent, sustained HTT protein reduction with subsequent suppression of mutant HTT aggregate formation in the striatum and cortex was found in Q175 mice. R6/2 mice showed functional improvement 8 weeks after AAV5-miHTT treatment. One-time AAV5-miHTT administration resulted in a median survival improvement of over 4 weeks compared with untreated R6/2 HD mice. Extensive human mutant HTT lowering, functional improvement, survival benefit, and tolerability of AAV5-miHTT support further development of our HTT-lowering gene therapy and initiation of clinical trials in HD patients in the near future.

RESULTS

One-Time Intrastriatal AAV5-miHTT Administration Results in Long-Term Expression of miHTT and Huntingtin Lowering in Q175 KI Mice

We have previously demonstrated strong suppression of HTT and improved neuropathology in HD rodents using miHTT, a miRNA targeting human *HTT* exon 1 expressed from a one-time delivery of AAV5 gene therapy.[17,18] The current studies were conducted to investigate the long-term expression and efficacy of miHTT in a mouse model of HD with a behavioral phenotype. In heterozygous Q175 KI mice, murine *HTT* exon 1 and part of intron 1 have been replaced with the human counterparts. Human exon 1 contains a large CAG repeat, which allows us to study the mechanism of action of AAV5-miHTT. To determine the long-term expression of the transgene and subsequent HTT lowering, adult Q175 KI heterozygous mice were injected bilaterally in the striatum with AAV5-miHTT at 5× increasing doses (n = 8, males only; low, medium, and high doses). Additional wild-type littermates and Q175 KI mice were injected with vehicle and served as control groups (Figure 1A). To evaluate any phenotypical changes, behavioral analyses were performed at several time points following administration of AAV5-miHTT. The behavioral analysis consisted of rotarod, open field, and fine motor analysis (MotoRater), evaluated every 3 months (Figure 1B). Twelve months after administration of AAV5-miHTT, the right hemisphere of the brain was taken from all animals to determine the level of vector DNA, transgene RNA, and HTT protein (Figure 1C). The striatum and cortex samples were used to determine the amount of HTT protein lowering to assess target

engagement. Distribution of the vector DNA and transgene expression were determined in cortex samples.

Vector DNA Distribution and Expression of the miRNA Targeting HTT mRNA in the Brain of Q175 KI Mice

The amount of vector DNA in the cortex of Q175 KI mice was determined by qPCR using primers designed specifically for the AAV5-miHTT expression cassette. Insufficient striatum tissue was available for this analysis because of the limited size of the mouse striatum. Even though the cortex was not the target region of the intrastriatal injection, dose-dependent levels of vector DNA were observed in the cortex of AAV5-miHTT-treated animals (Figure 2A). The low dose showed 1.3×10^4 vector genome copies (gc) per microgram genomic DNA (gDNA), whereas high-dose animals had values of up to 10^6 gc/μg gDNA. As expected, vehicle-treated animals gave values below background levels. The guide miHTT transgene (relative to vehicle-treated animals) was also dose-dependently expressed in the cortex of AAV5-miHTT-treated animals. Relative to vehicle-treated animals, expression of the transgene was, on average, 200-, 1,500-, and 4,000-fold higher in low-, medium-, and high-dose animals, respectively. Vector DNA levels significantly correlated with the level of miHTT expression in the cortex (Figure S1). Vector DNA as well as dose-dependent miHTT expression in the cortex were sustained 12 months after a striatal injection of AAV5-miHTT in Q175 mice. Because the miHTT transgene is expressed in the cortex, an area of the brain that was not the direct target of AAV5-miHTT administration, this indicated that the AAV5 vector was actively distributed via axonal transport through the brain.[16] GFP expression in mouse brains injected with AAV5-GFP following the same administration and dose range also shows dose-dependent widespread distribution of the vector transgene to the striatum and cortex (Figure S2).

Dose-Dependent Huntingtin Protein and Aggregate Lowering in the Brain of Heterozygous Q175 KI Mice

The striatum and cortex from the right hemisphere were used to determine the expression of soluble human mutant HTT protein. A significant dose-dependent average reduction of mutant HTT protein of up to 39% in the striatum and up to 13% in the cortex of Q175 KI mice 12 months after intrastriatal injection of AAV5-miHTT was detected (Figure 3A). The left hemisphere was used for EM48 staining
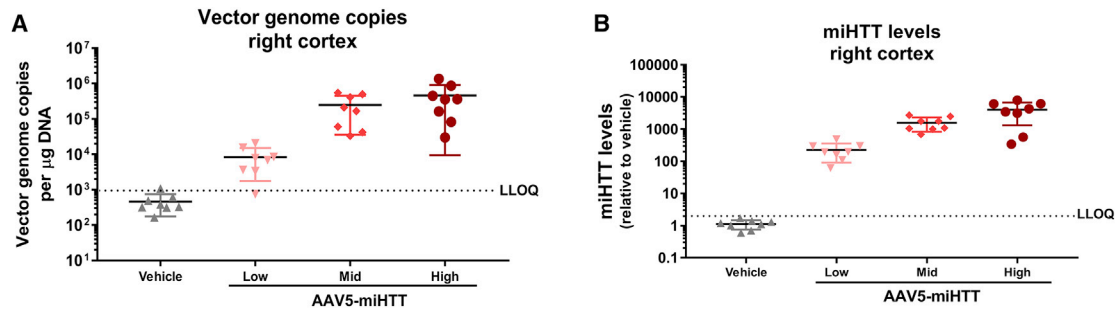
Figure 2. AAV5-miHTT Vector DNA Distribution and miHTT Expression 12 months after Striatal Injection in Q175 KI Brains
(A) Vector DNA copies (gc per microgram total genomic DNA) in the cortex collected from the right hemisphere of each animal (mean ± SEM). (B) Mature miHTT expression in the cortex from the right hemisphere was determined by custom TaqMan qRT-PCR. Values are represented as relative expression for each animal (mean ± SEM).

to determine the amount of mutant HTT aggregates in the striatum and cortex, the pathological hallmark of HD (Figure 3B). EM48 staining showed a reduction of HTT aggregates in the striatum and cortex of Q175 KI mice treated with the high dose compared with vehicle-treated Q175 KI mice (Figure 3C). Both the soluble HTT protein and the HTT aggregate analysis demonstrate that AAV5-miHTT leads to sustained HTT lowering and reduction of aggregation in a mouse model of HD.

No Clear Behavioral Phenotype in the Q175 KI Mouse Model

A rotarod and open field test were performed on Q175 KI mice and wild-type littermates before dosing (at 3 months of age) and at consecutive intervals 3, 6, and 9 months following administration of vehicle with AAV5-miHTT. Neither the rotarod nor the open field test showed a clear phenotype when comparing vehicle-treated Q175 KI mice with wild-type littermates (one-way ANOVA, Dunnett's *post hoc* test, $p > 0.05$) (Figure S3). This has been reported previously by others when using the heterozygous mouse model.[22] Fine motor skills and gait analyses were performed using the MotoRater, which records the complete movement of mice. Principal-component analysis of this gait analysis showed minimal and inconsistent differences between Q175 KI mice and wild-type littermates. Thus, because of a lack of gross motor phenotype development and absence of clear behavioral deficits in this Q175 heterozygous KI mouse model, an improvement by AAV5-miHTT treatment of these functional parameters could not be assessed in this study.

Long-Term Tolerability of AAV5-miHTT Treatment in Heterozygous Q175 KI Mice

AAV5-miHTT intrastriatal administration led to widespread distribution, long-term expression of therapeutic miHTT, dose-dependent knockdown of HTT protein, and a reduction in the number of HTT aggregates in both the striatum and cortex. Unfortunately, no phenotype was observed, so the effect of AAV5-miHTT on an HD-like phenotype could not be evaluated. Because the mice were followed for 1 year, we also investigated the tolerability of long-term AAV5-miHTT treatment. At necropsy, blood samples were used for clinical chemistry, and AAV5-miHTT treatment did not result in any changes in the parameters that were measured (Figure S4). The left

hemisphere of the brain and all major organs were collected and subjected to macroscopic and microscopic examination by a certified pathologist. This revealed no treatment-related findings in any of the organs, including the brain, after H&E staining (data not shown). Although heterozygous Q175 KI mice did not develop a clear HD-like phenotype, AAV5-miHTT treatment did not trigger any behavioral deficits. In conclusion, investigations looking into the tolerability of long-term high-vector DNA and miHTT expression show no tolerability issues up to 1 year after the initial treatment.

Intrastriatal AAV5-miHTT Administration Results in Functional and Survival Improvement in R6/2 Mice

Because Q175 KI HD mice did not develop a clear HD-like phenotype, the effect of AAV5-miHTT treatment on the functional improvement of HD-like symptoms was investigated in a follow-up study in R6/2 HD mice. The R6/2 mouse was selected for the rapid phenotype and because this model expresses the expanded exon 1 of the human HTT gene, including the target site of miHTT.[15] This mouse model is known for showing symptoms as early as 6–8 weeks of age and has a median survival of approximately 16 weeks.[23] R6/2 mice were injected at 4 weeks of age with AAV5-miHTT using the same procedure and doses as for the Q175 KI mouse study and were followed for up to 5 months (Figure 4A). Behavior testing in the form of rotarod and evaluation of the clasping phenotype were performed at several time points during the in-life phase (Figure 4B).

R6/2 mice are known to have impaired body weight gain during their lifespan, and in the current study, R6/2 mice started losing body weight around 10 weeks of age (Figure S5). Starting at 11 weeks of age, R6/2 mice also had increased mortality, and, consequently, the number of animals per group decreased over time. Treatment with the high dose of AAV5-miHTT resulted in a significantly higher body weight in R6/2 mice compared with untreated R6/2 mice at 10, 11, 13, 15–19, and 21 weeks of age (one-way ANOVA, $p < 0.05$) (Figure 5).

R6/2 mice lose motor coordination over time, and this can be monitored using the rotarod test.[21] The resulting phenotype in this model becomes severe around 8–12 weeks of age.[15] In our study, the rotarod
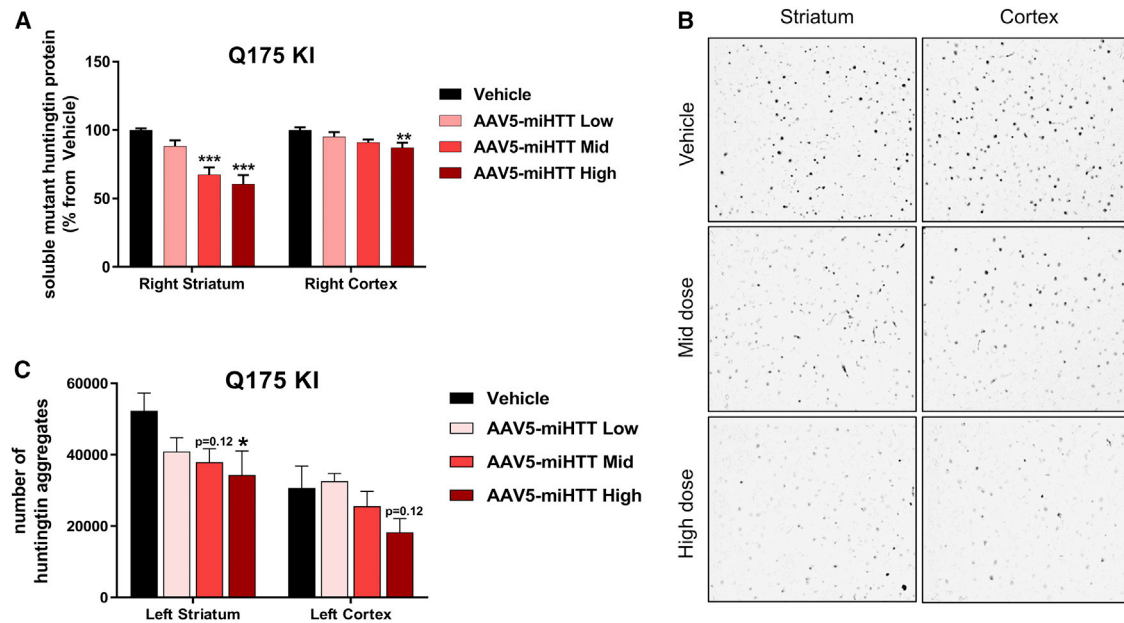
Figure 3. AAV5-miHTT Treatment Demonstrates Human Mutant Huntingtin Target Engagement in Q175 KI Mouse Striatum and Cortex

(A) MSD quantification of soluble human mutant huntingtin protein levels in the striatum and cortex from the right hemisphere (mean ± SEM). Data were evaluated using ordinary one-way ANOVA. **$p < 0.01$, ***$p < 0.001$. (B) Immunohistochemistry staining of the striatum and cortex from the left hemisphere using the EM48 antibody, which is specific for mutant huntingtin protein. (C) Quantification of mEM48 staining of the striatum and cortex (mean ± SEM). Data were evaluated using ordinary one-way ANOVA. *$p < 0.05$.

test was performed at week 0 (pre-dose) and 4 and 8 weeks after treatment with AAV5-miHTT. A decreased latency to fall was already observed in vehicle-treated R6/2 mice at 8 weeks of age (Figure 6A), and at 12 weeks of age, this difference was even more pronounced. AAV5-miHTT treatment showed a significant improvement in motor coordination on the rotarod by an increase in latency to fall of 22 s in the high-dose group, which is an increase of 56% compared with vehicle-treated R6/2 mice (one-way ANOVA, p = 0.0226; Figure 6B).

Wild-type animals spread out their limbs when they are picked up by the tail, whereas R6/2 mice are known for clasping their hind- and frontlimbs tightly against their body because of their motor deficits.[21] Both the time until the hindlegs touched each other and the time until full clasping of the hindlegs were recorded for 5 animals per group. A dose-dependent trend of increasing time to touch the hindlegs and to clasping was observed in AAV5-miHTT treated animals compared with vehicle-treated R6/2 mice at 12 weeks of age, but these results did not reach significance (Figure 6C) (one-way ANOVA).

The average lifespan of a wild-type mouse is approximately 2 years, whereas R6/2 mice have a median survival of 16 weeks, with increased mortality starting at 10 weeks of age.[21] One-time bilateral intrastriatal injection of both the low and high dose of AAV5-miHTT resulted in a significant increase in median survival compared with vehicle-treated R6/2 HD mice (Figure 7). Treating R6/2 mice with a low dose increased the median survival by 26.5 days (p = 0.035), whereas the

high dose showed an increase of 29 days (median, 149 days; p = 0.0292) compared with untreated R6/2 mice, which had a median survival of 120 days.

The R6/2 mice used in the study showed a strong phenotype based on body weight, motor coordination, behavior, and survival endpoints compared with their wild-type littermates. Our data show that treatment with AAV5-miHTT led to significant improvements in body weight and behavior and increased survival, partially correcting the severe HD-like phenotype.

DISCUSSION

The present study shows that targeting human HTT mRNA is effective in lowering the soluble mutant HTT protein and reducing the amount of HTT aggregates in the brain in a relevant murine model of HD. Intrastriatal administration of AAV5-miHTT resulted in therapeutic miRNA expression throughout the murine brain and HTT protein lowering in both the cortex and striatum in the Q175 HD mouse model. This is in agreement with our previous publication, where it was shown that AAV5-miHTT suppressed *HTT* mRNA and prevented the formation of mutant HTT aggregate formation, which led to suppression of DARPP-32-associated neuronal dysfunction in a HD rat model.[18] The current studies confirm HTT protein lowering in the CNS up to 12 months after treatment. The HTT lowering is not as strong as might be expected, most likely because of differences between the assays and because the entire brain structures were used, which can dilute the effect. Nevertheless, there is still
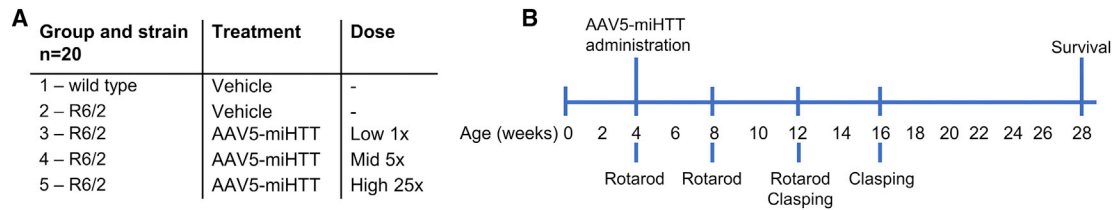
Figure 4. AAV5-miHTT Administration in the Mouse Brain Using a Single Bilateral Intrastriatal Stereotactic Injection
(A) Experimental setup, showing wild-type and R6/2 mice used in the study with the different dose groups. (B) Experimental setup; n = 20 per group. Behavioral tests were performed to assess motor skills at several time points as indicated. Dosing (at 4 weeks of age) and scheduled necropsy of surviving mice (at 28 weeks of age) are indicated.

an almost 40% reduction of HTT protein in the striatum. In addition, we have shown functional improvement in a severe mouse model for HD after treatment with AAV5-miHTT, which is seen in the rotarod test, body weight, and improved median survival in the R6/2 mouse model.

The heterozygous Q175 KI model was chosen for our study because the model contains an expanded CAG repeat within one of the native mouse HTT genes that mimics the mutation found in HD patients and is therefore a reliable measure of HTT suppression. However, recently it has been shown that this model does not show a robust HD-like phenotype.[24,25] A newer model, the Q175FDN mouse, has been recommended as a more relevant HD model.[22] Hence, heterozygous Q175 mice could not be used for evaluation of motor function defects and phenotype improvement by AAV5-miHTT treatment. However, the study does show that one-time intrastriatal administration of AAV5-miHTT resulted in dose-dependent lowering of HTT protein 12 months following treatment. This reduction of mutant HTT was observed both in the cortex and the striatum and resulted in a reduction of the number of HTT aggregates. For this analysis, a homogenized sample from each structure was used to determine the level of HTT protein. This does not allow determination of HTT protein levels in a specific brain area and could dilute the actual HTT-lowering effect in some areas, particularly in the cortex. The safety of AAV5-miHTT treatment and consequent HTT lowering was also evaluated in this study, and no adverse effects, effects on clinical chemistry, or histopathological changes in any of the major organs, including the brain, were found, indicating long-term tolerability of one-time administration of AAV5-miHTT to the striatum. Total HTT lowering in the brain has been shown to be well-tolerated in adult mice,[26] and total knockdown of HTT in the striatum and cerebral cortex, followed for 14 months, also did not lead to obvious pathology.[27]

For translatability to the clinic, we performed a study in transgenic HD minipigs also utilizing intracranial administration of AAV5-miHTT.[19] We described previously that treatment was well-tolerated, and no histological pathology was found. Widespread vector distribution and miHTT expression were found throughout the minipig brain. A clear trend toward dose-dependent reduction of human mutant HTT was shown, with up to 85% lowering. The larger size and complexity of the minipig brain compared with rodents allows

better translatability of the AAV5-miHTT treatment to the clinic. R6/2 mice express a truncated mutant HTT cDNA fragment, resulting in CNS as well as systemic pathology and a greatly reduced lifespan. R6/2 mice start dying around 10 weeks of age, with median death between 14–18 weeks.[21] The initial onset of motor symptoms signals is around 3 weeks of age,[15] and mice in this study were injected with AAV5-miHTT at 4 weeks of age, during the symptomatic phase. In the current study, all groups treated with AAV5-miHTT (single intrastriatal injection) had increased survival compared with the vehicle group. The median survival was significantly improved by 29 days in the high-dose group. In a previously reported study with intracerebroventricular infusions of ASOs targeting HTT mRNA, 23-day improvement in median survival was shown after daily treatments with a high total dose of ASOs.[4] Another proposed therapeutic agent for HD, a p75 neurotrophin receptor ligand, LM11A-31, demonstrated an increase in mean survival of 17 days in R6/2 mice.[28] Many other studies have not investigated or reported survival[29,30] or failed to see an improvement in survival after treatment.[31,32]

Because the R6/2 mouse model displays a clear motor phenotype, this has been used a functional outcome measure in many studies. Eight weeks after AAV5-miHTT treatment, the high-dose group showed a 56% rotarod improvement compared with control animals. The rotarod test could not be performed at later time points because this would have been too strenuous for the mice. Other studies have also shown rotarod improvement, such as a 30% rotarod improvement 1 week after neural stem cell transplantation[30] and rotarod improvement in all dose groups 7 to 8 weeks after laquinimod treatment at 12 weeks of age.[32] One of the phenotypes found in several HD mouse models that express a partial human HTT fragment is decreased body weight. Most studies using R6/2 mice did not find a positive effect on body weight.[28,30,32,33] In the current study, there was a significant beneficial effect on body weight in R6/2 mice at several time points after treatment with AAV5-miHTT. Several different therapies (ASO,[4] laquinimod,[32] and LM11A-31[28]) that are currently used in clinical trials have all shown some survival or behavioral improvement in R6/2 mice, but this was not as strong as in the present study.

Altogether, the data from the current studies corroborate and extend the strong evidence of therapeutic efficacy of the AAV5-miHTT vector by inducing sustained HTT protein lowering in the brain.
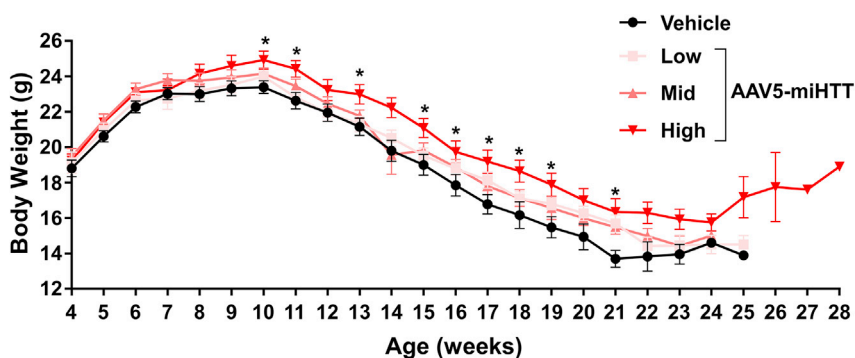
Figure 5. Body Weight Development over Time in R6/2 Mice

AAV5-miHTT treatment at the high dose shows significantly higher body weight in R6/2 mice compared with untreated R6/2 mice at several time points between 10 and 21 weeks of age (shown as asterisks in the graph).

AAV5-miHTT-mediated HTT lowering resulted in functional improvement in a severe mouse model for HD. It was shown that, even up to 12 months after a single treatment with AAV5-miHTT, significantly lowered HTT protein levels were observed without raising any safety concerns. The phenotypical improvement in R6/2 mice was seen both in a significant increase in median survival and in motor function, as demonstrated by rotarod testing. The sustained human mutant HTT lowering, functional improvement, survival benefit, and tolerability of AAV5-miHTT support further development of HTT-lowering gene therapy and initiation of clinical trials in HD patients in the near future.

MATERIALS AND METHODS

Animals

All procedures were carried out in accordance with the European Community Directive (86/609/EEC) for the Care and Use of Laboratory Animals, using protocols approved and monitored by the Animal Experiment Board of Finland. Heterozygous Q175 KI R6/2 mice and their wild-type littermates were bred by Charles River Laboratories (Germany) and genotyped at weaning. Animals were housed in a temperature-controlled room and maintained on a 12-h day and night cycle. Food and water were available *ad libitum*.

AAV5-miHTT

The AAV5 vector encoding cDNA of the miHTT cassette was produced using a baculovirus-based AAV production system (uniQure, Amsterdam, the Netherlands) as described previously.[17] Expression was driven by a combination of the cytomegalovirus early enhancer element and chicken β-actin promoter, and the transcription unit was flanked by two non-coding AAV-derived inverted terminal repeats.

Surgical Procedures

Standard aseptic surgical procedures were used to perform the injections. Briefly, mice were anesthetized with 5% isoflurane and placed in a stereotactic frame. During the operation, the concentration of anesthetic was reduced to 1.0%–1.5%. 2 μL of vehicle or AAV5-miHTT was injected into the striatum in both hemispheres (anterior-posterior [AP], +0.8 mm; medial-lateral [ML], ±1.8 mm; dorsal-ventral [DV], −3.0 mm) using a 10-μL Hamilton syringe at a rate of

0.4 μL/min. The needle was left in place for 3 min after surgery, retracted by 1 mm, and left for another 3 min, and then the needle was removed completely. One hour before and for 48 h after surgery, mice were administered buprenorphine (Temgesic, 0.03 mg/kg, 1 mL/kg subcutaneously) for analgesia.

Animal Perfusion and Tissue Collection

All of the Q175 KI and wild-type mice and the R6/2 mice that were alive until 28 weeks of age were euthanized at the end of the study. The mice were perfused with ice-cold heparinized saline after the brain was removed, and the right cortex and striatum were collected and frozen in liquid nitrogen and kept at −80°C until further analysis. The left hemisphere of the brain was stored in 4% paraformaldehyde (PFA) for further analysis.

Clinical Chemistry

Clinical biochemistry panels of markers were analyzed in non-hemolyzed serum for the following parameters: alkaline phosphatase (AFOS), alanine aminotransferase (ALAT), aspartate aminotransferase (ASAT), albumin (ALB), gamma-glutamyl transferase (GGT), creatinine (Crea), total protein (Prot), urea (UREA), calcium (Ca), cholesterol (Chol), and inorganic phosphate (Pi).

qPCR DNA and RNA

Q175 KI mouse and wild-type littermate brain samples from the right cortex were used for DNA and RNA isolation, and levels were measured by qPCR.

Tissue was crushed using the CryoPrep system (Covaris, Woburn, MA, USA), and the powder was divided for DNA and RNA analysis. DNA was extracted from pulverized cortex tissue with the DNAeasy 96 Blood and Tissue Kit (QIAGEN, Germany). Primers specific for the CAG promoter were used to amplify a sequence specific for the transgenes by SYBR Green Fast qPCR (Thermo Fisher Scientific). The genome copies per microgram of genomic DNA (gDNA) input of the samples were calculated by interpolation of a standard line of the expression cassette. To define the background levels of the qPCR, a blank sample was subjected to qPCR using the same expression cassette targeting primers.

Total RNA was extracted from crushed cortex tissue and used to determine the level of miHTT (microRNA expression) and HTT mRNA expression (the target). For miHTT miRNA expression, RNA was used to reverse-transcribe RNA into cDNA using a gene-specific RT-PCR using a stem-loop RT primer specifically targeting
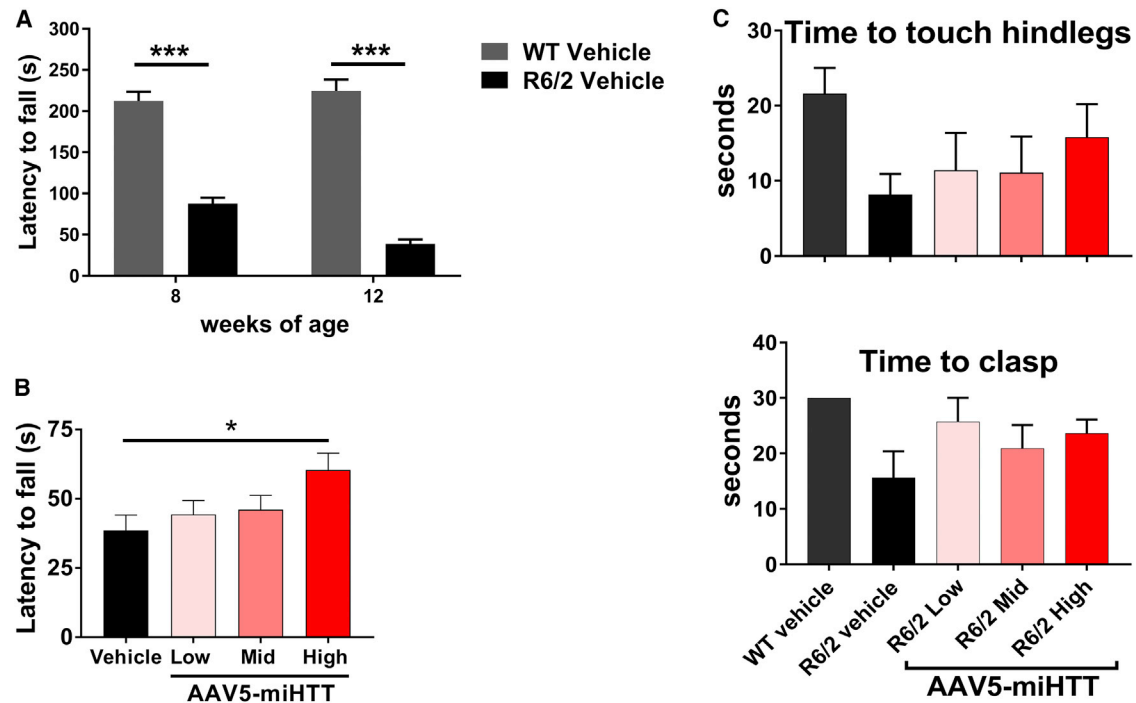
Figure 6. AAV5-miHTT Treatment Shows Motor Coordination Improvement in R6/2 Mice

(A) Untreated R6/2 mice had a significantly lower latency to fall on the rotarod compared with wild-type littermates. (B) An increase in latency to fall of 47% was found in R6/2 mice treated with a high dose of AAV5-miHTT (mean ± SEM, p < 0.05). (C) Videos from 5 animals per group were scored for the time to touch and time to clasp hindlegs. Even though there was no significant effect, both parameters show a trend toward the wild-type animals after AAV5-miHTT treatment (mean ± SEM).

the miHTT. Each cDNA sample was subjected to TaqMan qPCR using a primer-probe set specific for miHTT and an internal control miRNA (U6). Mature miHTT levels in the samples were calculated by normalized control miRNA and relative to the vehicle control Q175 KI group. To control for gDNA contamination in the samples, an RT and no-template control sample were subjected to qPCR using the same primer-probe set specific for miHTT.

Total RNA was treated with DNase (Thermo Scientific, Waltham, MA, USA) to remove gDNA and reverse-transcribed into cDNA using a DyNAmo cDNA Synthesis Kit (Thermo Fisher Scientific, F-470L) following the manufacturer's instructions. Each cDNA sample was subjected to TaqMan qPCR using a primer-probe set targeting human *HTT* and an internal control housekeeping gene (*Gapdh*). Human *HTT* expression levels were calculated by normalizing to the housekeeping gene and relative to the average of the Q175 KI vehicle control group based on the $2^{-\Delta\Delta Ct}$ method[34]. To control for DNase treatment efficacy and efficiency and potential gDNA contamination in the samples, RT, DNase, RT-DNase+, and no-template control samples were subjected to qPCR using the same primer-probe set specific for human *HTT*.

The RT reaction was performed on a Biometra GMBHT advanced thermocycler, and qPCR runs were performed on an ABI-7500 fast real-time qPCR cycler.

HTT Protein Expression in Brain Tissue Homogenates

Quantification of mutant HTT protein in heterozygous Q175 mouse brain samples was performed at Evotec (Hamburg, Germany) using a customized mesoscale discovery (MSD) assay. Pulverized brain samples were homogenized in 170 μL ice-cold lysis buffer (Dulbecco's PBS, 0.4% Triton X-100, and protease and phosphatase inhibitor) using a FastPrep24 tissue homogenizer. The homogenates were aliquoted, frozen on dry ice, and stored at −80°C until further use. With one aliquot, the total protein concentration was determined by bicinchoninic acid assay (BCA). For the MSD assay, the homogenates were first diluted to 0.2 mg/mL total protein with lysis buffer and then 1:2 with MSD blocking buffer. From this dilution, technical triplicates were measured on one assay plate in MSD. The MSD plate was coated with the capture antibody 2B7 (5 μg/mL in MSD coating buffer), and detection of expanded HTT was carried out with sulfo tag-labeled MW1 detection antibody (5 μg/mL in MSD blocking buffer). In parallel with the tissue homogenates, the following recombinant standard protein was used for quantification: human HTT-Q46_GST, 1-548 (EV4238) diluted with lysis buffer and spiked into wild-type mouse brain homogenate (0.2 mg/mL in MSD blocking buffer). Standard protein was applied at a final assay concentration range between 0.04 and 2,100 ng/mL. Finally, 1× MSD read buffer was pipetted to the assay plate, and the plate was read with Mesoscale Imager SI6000. The standard curve was used to extrapolate the levels of mutant HTT protein and
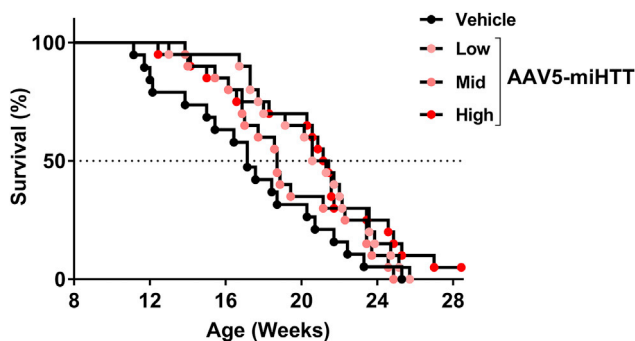
Figure 7. Kaplan-Meier Curve Showing Survival of Untreated and AAV5-miHTT-Treated R6/2 Mice

Median survival was increased significantly in the low- and high-dose groups (26.5 and 29 days, respectively; p < 0.05).

subsequently corrected by the micrograms of total protein in the sample.

Immunohistochemistry

The left hemisphere of the brain was embedded in paraffin, and sections were processed for immunostaining with EM48, an antibody specific for aggregated HTT.[35] The brains were cut into 20-μm-thick sections at 200-μm intervals, mounted on slides, and stored at −80°C until use for immunostaining. First, paraffin was removed from the slides with Roti-clear and a descending alcohol series. This was followed by incubation with 0.01 M citric acid at 80°C. Sections were then washed with Tris-buffered saline tween (TBS-T) twice for 5 min each, and all sections were then permeabilized and blocked with 3% BSA and 10% normal goat serum (NGS) containing 0.3% Triton X-100 in Tris-buffered saline (TBS) for 30 min. Sections were washed with 3% BSA for 5 min, incubated with EM48 primary antibody (mouse anti-mutant HTT inclusion, mEM48; Millipore, MAB5374; dilution, 1:500) overnight at room temperature before washing them with TBS three times for 10 min each. Secondary antibody incubation (biotinylated goat anti-mouse; vector BA-9200; dilution, 1:500) was done for 2 h at room temperature. All sections were then washed with TBS three times for 5 min each.

All sections were then incubated with a peroxidase avidin-biotin complex (vector PK-6100; dilution, 1:500) for 2 h at room temperature. After washing in PBS three times for 5 min each, 3,3'-diaminobenzidine (DAB) was used as a substrate, the reaction was monitored by visual inspection of the color formation for a few minutes, and then H_2O was used to stop the reaction. Finally, the sections were dehydrated and mounted with Roti-Mount mounting medium (Carl Roth). Representative images of the striatum and motor cortex were taken using an Axio Imager.M2 microscope (Zeiss, Germany) using an EC Plan-Neofluar 20× objective (N.A., 0.5; W.D., ∞) and an EC Plan-Neofluar 40× objective (N.A., 0.75; W.D., ∞) (Carl Zeiss). Images for EM48 were analyzed for the number of aggregates per area in the cortical and striatal regions. Image analysis was performed using a particle count macro written for ImageJ software.

The striatum and motor cortex were delineated manually from each analyzed section. Then the delineated area (total area) was thresholded by visual inspection to highlight any positive staining found within the region of interest (ROI). Positively stained aggregates were detected and counted, and the number of aggregates per area was calculated.

For GFP staining, the brains were embedded in paraffin. From these blocks, sections of 4 μM were cut with the microtome and mounted on slides. After drying the slides overnight, the sections were dewaxed and rehydrated. Tissue sections were blocked with PBS+5% BSA+5% NGS to prevent background staining, followed by overnight incubation at 4°C with anti-GFP (ab290, 1:1,000). On the second day, the sections were with treated with 1% H_2O_2+30% ethanol+PBS to inactivate endogenous peroxidase. Rabbit Envision (Dako) was applied on the sections for 30 min. The staining was developed with a DAB substrate kit (Abcam, ab64238), and images were acquired on a Leica Aperio Versa 8.

Behavioral Analysis
Accelerating Rotarod Test

Q175 mice were tested at 3 months of age (pre-treatment baseline) and 3, 6, and 9 months after dosing. R6/2 mice were tested at 4 weeks of age (pre-treatment baseline) and 4 and 8 weeks after dosing. The rotarod test was performed during the light phase of the animals. Each session included a training trial of 5 min at 4 rpm on the rotarod apparatus (AccuScan Instruments, Columbus, OH, USA). After the training trial, the animals were tested for 3 consecutive accelerating trials of 6 min, with the speed changing from 0 to 40 rpm over 360 s and an inter-trial interval of at least 30 min. The latency to fall from the rod was recorded. Mice remaining on the rod for more than 360 s were removed, and their time was scored as 360 s.

Open Field Test

Q175 mice were tested at 3 months of age (pre-treatment baseline) and 3, 6, and 9 months after dosing. The mice were brought to the experimental room for at least 1 h of acclimation to the experimental room conditions prior to testing. The open field test was performed during the early nocturnal phase of the animals. Activity chambers (Med Associates, St. Albans, VT, USA; 27 × 27 × 20.3 cm) were equipped with infrared (IR) beams. Mice were placed in the center of the chamber, and their behavior was recorded for 30 min in 5-min bins. Quantitative analysis was performed on the following five dependent measures: total locomotion, locomotion in the center of the open field, rearing rate in the center, total rearing frequency, and velocity. Animals were tested under low-stress conditions, where the light was lowered to approximately 10–30 lux of red light.

MotoRater

The fine motor skills and gait of Q175 mice were measured in the MotoRater (TSE Systems, Bad Homburg, Germany) 6 and 9 months after dosing during the light phase. Prior to the test, the mice were shaved under light isoflurane anesthesia, and the essential body points were marked for tracking.

The data regarding gait performance were captured using a camera with a speed of 300 frames/s, imaging the gait from three different views (below and both sides). The captured videos of each mouse were first converted to SimiMotion software to track the marked points of the body from the video, obtaining raw data for analysis. The raw data thus comprised the movements of different body points in coordinates related to the ground and each of the three dimensions.

Different gait patterns and movements were analyzed using a custom-made automated analysis system. The data were then analyzed regarding several specific clusters of parameters, and all fine motor data were analyzed for 97 distinctive parameters. The parameter data were further processed using principal-component analysis (PCA).

Video Analysis
This analysis was done on R6/2 mice at 12 weeks of age during the light phase. Per group, 5 animals were filmed to observe clasping behavior. The mice were picked up by the tail for approximately 30 s to induce the clasping behavior. Two individual observers scored the videos for the time it took the mice to touch the hindlegs together and the time it took until the hindlegs were fully clasping.

Statistics
Mean values were used for statistical analyses. Data are expressed as means ± SEM. Student's t test was used for statistical comparison between two groups.

For comparisons of more than two groups, one-way ANOVA was used, followed by Dunnett's-Tukey's multiple comparisons *post hoc* test (Prism, GraphPad, San Diego, CA, USA). For both tests, $p < 0.05$ was considered a statistically significant difference.

SUPPLEMENTAL INFORMATION
Supplemental Information can be found online at https://doi.org/10.1016/j.omtm.2019.03.002.

REFERENCES
1. Ross, C.A., and Tabrizi, S.J. (2011). Huntington's disease: from molecular pathogenesis to clinical treatment. Lancet Neurol. 10, 83–98.
2. Vonsattel, J.P., and DiFiglia, M. (1998). Huntington disease. J. Neuropathol. Exp. Neurol. 57, 369–384.
3. Melone, M.A., Jori, F.P., and Peluso, G. (2005). Huntington's disease: new frontiers for molecular and cell therapy. Curr. Drug Targets 6, 43–56.
4. Kordasiewicz, H.B., Stanek, L.M., Wancewicz, E.V., Mazur, C., McAlonis, M.M., Pytel, K.A., Artates, J.W., Weiss, A., Cheng, S.H., Shihabuddin, L.S., et al. (2012). Sustained therapeutic reversal of Huntington's disease by transient repression of huntingtin synthesis. Neuron 74, 1031–1044.
5. Ross, C.A., Aylward, E.H., Wild, E.J., Langbehn, D.R., Long, J.D., Warner, J.H., Scahill, R.I., Leavitt, B.R., Stout, J.C., Paulsen, J.S., et al. (2014). Huntington disease: natural history, biomarkers and prospects for therapeutics. Nat. Rev. Neurol. 10, 204–216.
6. Aronin, N., and DiFiglia, M. (2014). Huntingtin-lowering strategies in Huntington's disease: antisense oligonucleotides, small RNAs, and gene editing. Mov. Disord. 29, 1455–1461.
7. Godinho, B.M., Malhotra, M., O'Driscoll, C.M., and Cryan, J.F. (2015). Delivering a disease-modifying treatment for Huntington's disease. Drug Discov. Today 20, 50–64.
8. Stanek, L.M., Sardi, S.P., Mastis, B., Richards, A.R., Treleaven, C.M., Taksir, T., Misra, K., Cheng, S.H., and Shihabuddin, L.S. (2014). Silencing mutant huntingtin by adeno-associated virus-mediated RNA interference ameliorates disease manifestations in the YAC128 mouse model of Huntington's disease. Hum. Gene Ther. 25, 461–474.
9. Coffey, S.R., Bragg, R.M., Minnig, S., Ament, S.A., Cantle, J.P., Glickenhaus, A., Shelnut, D., Carrillo, J.M., Shuttleworth, D.D., Rodier, J.A., et al. (2017). Peripheral huntingtin silencing does not ameliorate central signs of disease in the B6.HttQ111/+ mouse model of Huntington's disease. PLoS ONE 12, e0175968.
10. van Roon-Mom, W.M.C., Roos, R.A.C., and de Bot, S.T. (2018). Dose-Dependent Lowering of Mutant Huntingtin Using Antisense Oligonucleotides in Huntington Disease Patients. Nucleic Acid Ther. 28, 59–62.
11. Boudreau, R.L., Rodríguez-Lebrón, E., and Davidson, B.L. (2011). RNAi medicine for the brain: progresses and challenges. Hum. Mol. Genet. 20 (R1), R21–R27.
12. Srivastava, A. (2016). In vivo tissue-tropism of adeno-associated viral vectors. Curr. Opin. Virol. 21, 75–80.
13. Markakis, E.A., Vives, K.P., Bober, J., Leichtle, S., Leranth, C., Beecham, J., Elsworth, J.D., Roth, R.H., Samulski, R.J., and Redmond, D.E., Jr. (2010). Comparative transduction efficiency of AAV vector serotypes 1-6 in the substantia nigra and striatum of the primate brain. Mol. Ther. 18, 588–593.
14. Burger, C., Gorbatyuk, O.S., Velardo, M.J., Peden, C.S., Williams, P., Zolotukhin, S., Reier, P.J., Mandel, R.J., and Muzyczka, N. (2004). Recombinant AAV viral vectors pseudotyped with viral capsids from serotypes 1, 2, and 5 display differential efficiency and cell tropism after delivery to different regions of the central nervous system. Mol. Ther. 10, 302–317.
15. Li, J.Y., Popovic, N., and Brundin, P. (2005). The use of the R6 transgenic mouse models of Huntington's disease in attempts to develop novel therapeutic strategies. NeuroRx 2, 447–464.
16. Samaranch, L., Blits, B., San Sebastian, W., Hadaczek, P., Bringas, J., Sudhakar, V., Macayan, M., Pivirotto, P.J., Petry, H., and Bankiewicz, K.S. (2017). MR-guided parenchymal delivery of adeno-associated viral vector serotype 5 in non-human primate brain. Gene Ther. 24, 253–261.
17. Miniarikova, J., Zanella, I., Huseinovic, A., van der Zon, T., Hanemaaijer, E., Martier, R., Koornneef, A., Southwell, A.L., Hayden, M.R., van Deventer, S.J., et al. (2016). Design, Characterization, and Lead Selection of Therapeutic miRNAs Targeting Huntingtin for Development of Gene Therapy for Huntington's Disease. Mol. Ther. Nucleic Acids 5, e297.
18. Miniarikova, J., Zimmer, V., Martier, R., Brouwers, C.C., Pythoud, C., Richetin, K., Rey, M., Lubelski, J., Evers, M.M., van Deventer, S.J., et al. (2017). AAV5-miHTT gene therapy demonstrates suppression of mutant huntingtin aggregation and neuronal dysfunction in a rat model of Huntington's disease. Gene Ther. 24, 630–639.

19. Evers, M.M., Miniarikova, J., Juhas, S., Valles, A., Bohuslavova, B., Juhasova, J., Skalnikova, H.K., Vodicka, P., Valekova, I., Brouwers, C., et al. (2018). AAV5-miHTT Gene Therapy Demonstrates Broad Distribution and Strong Human Mutant Huntingtin Lowering in a Huntington's Disease Minipig Model. Mol. Ther. 26, 2163–2177.

20. Menalled, L.B., Kudwa, A.E., Miller, S., Fitzpatrick, J., Watson-Johnson, J., Keating, N., Ruiz, M., Mushlin, R., Alosio, W., McConnell, K., et al. (2012). Comprehensive behavioral and molecular characterization of a new knock-in mouse model of Huntington's disease: zQ175. PLoS ONE 7, e49838.

21. Mangiarini, L., Sathasivam, K., Seller, M., Cozens, B., Harper, A., Hetherington, C., Lawton, M., Trottier, Y., Lehrach, H., Davies, S.W., and Bates, G.P. (1996). Exon 1 of the HD gene with an expanded CAG repeat is sufficient to cause a progressive neurological phenotype in transgenic mice. Cell 87, 493–506.

22. Southwell, A.L., Smith-Dijak, A., Kay, C., Sepers, M., Villanueva, E.B., Parsons, M.P., Xie, Y., Anderson, L., Felczak, B., Waltl, S., et al. (2016). An enhanced Q175 knock-in mouse model of Huntington disease with higher mutant huntingtin levels and accelerated disease phenotypes. Hum. Mol. Genet. 25, 3654–3675.

23. Ferrante, R.J. (2009). Mouse models of Huntington's disease and methodological considerations for therapeutic trials. Biochim. Biophys. Acta 1792, 506–520.

24. Wheeler, V.C., Auerbach, W., White, J.K., Srinidhi, J., Auerbach, A., Ryan, A., Duyao, M.P., Vrbanac, V., Weaver, M., Gusella, J.F., et al. (1999). Length-dependent gametic CAG repeat instability in the Huntington's disease knock-in mouse. Hum. Mol. Genet. 8, 115–122.

25. White, J.K., Auerbach, W., Duyao, M.P., Vonsattel, J.P., Gusella, J.F., Joyner, A.L., and MacDonald, M.E. (1997). Huntingtin is required for neurogenesis and is not impaired by the Huntington's disease CAG expansion. Nat. Genet. 17, 404–410.

26. Wang, G., Liu, X., Gaertig, M.A., Li, S., and Li, X.J. (2016). Ablation of huntingtin in adult neurons is nondeleterious but its depletion in young mice causes acute pancreatitis. Proc. Natl. Acad. Sci. USA 113, 3359–3364.

27. Dietrich, P., Johnson, I.M., Alli, S., and Dragatsis, I. (2017). Elimination of huntingtin in the adult mouse leads to progressive behavioral deficits, bilateral thalamic calcification, and altered brain iron homeostasis. PLoS Genet. 13, e1006846.

28. Simmons, D.A., Belichenko, N.P., Ford, E.C., Semaan, S., Monbureau, M., Aiyaswamy, S., Holman, C.M., Condon, C., Shamloo, M., Massa, S.M., and Longo, F.M. (2016). A small molecule p75NTR ligand normalizes signalling and reduces Huntington's disease phenotypes in R6/2 and BACHD mice. Hum. Mol. Genet. 25, 4920–4938.

29. Datson, N.A., González-Barriga, A., Kourkouta, E., Weij, R., van de Giessen, J., Mulders, S., Kontkanen, O., Heikkinen, T., Lehtimäki, K., and van Deutekom, J.C. (2017). The expanded CAG repeat in the huntingtin gene as target for therapeutic RNA modulation throughout the HD mouse brain. PLoS ONE 12, e0171127.

30. Reidling, J.C., Relaño-Ginés, A., Holley, S.M., Ochaba, J., Moore, C., Fury, B., Lau, A., Tran, A.H., Yeung, S., Salamati, D., et al. (2018). Human Neural Stem Cell Transplantation Rescues Functional Deficits in R6/2 and Q140 Huntington's Disease Mice. Stem Cell Reports 10, 58–72.

31. Paré, M.F., and Jasmin, B.J. (2017). Chronic 5-Aminoimidazole-4-Carboxamide-1-β-d-Ribofuranoside Treatment Induces Phenotypic Changes in Skeletal Muscle, but Does Not Improve Disease Outcomes in the R6/2 Mouse Model of Huntington's Disease. Front. Neurol. 8, 516.

32. Ellrichmann, G., Blusch, A., Fatoba, O., Brunner, J., Hayardeny, L., Hayden, M., Sehr, D., Winklhofer, K.F., Saft, C., and Gold, R. (2017). Laquinimod treatment in the R6/2 mouse model. Sci. Rep. 7, 4947.

33. Zimmermann, T., Remmers, F., Lutz, B., and Leschik, J. (2016). ESC-Derived BDNF-Overexpressing Neural Progenitors Differentially Promote Recovery in Huntington's Disease Models by Enhanced Striatal Differentiation. Stem Cell Reports 7, 693–706.

34. Pfaffl, M.W. (2001). A new mathematical model for relative quantification in real-time RT-PCR. Nucleic Acids Res. 29, e45.

35. Gutekunst, C.A., Li, S.H., Yi, H., Mulroy, J.S., Kuemmerle, S., Jones, R., Rye, D., Ferrante, R.J., Hersch, S.M., and Li, X.J. (1999). Nuclear and neuropil aggregates in Huntington's disease: relationship to neuropathology. J. Neurosci. 19, 2522–2534.